SIMULATION OF STRONG EARTHQUAKE MOTIONS FOR INELASTIC STRUCTURAL RESPONSE

by

H. Kameda[I] and A. H-S. Ang[II]

SYNOPSIS

A method for simulating earthquake motion suitable for inelastic structural response is developed. Simulated accelerograms are generated so that deformation spectra and total hysteretic energy for elastoplastic systems will agree, in the mean, with corresponding recorded accelerograms. For this purpose, the equivalent duration and optimum spectral function of the simulated accelerograms are required; determination of these parameters are discussed.

INTRODUCTION

It is generally recognized that ground motions in a strong earthquake are random processes, and various stochastic models (1,2,3) have been proposed for this purpose. These have proved successful in the sense that both simulated and recorded accelerograms result in similar linear response spectra. However, agreement in the linear response spectra does not constitute a basis for the applicability of the models for inelastic response analysis. The objective of this study is the development of stochastic models for simulating strong earthquake motions for the purpose of inelastic structural response analysis and design.

For this purpose, appropriate definition of the duration of earthquake motion is required, since the inelastic structural response will be affected significantly by the duration of excitation. In this study, the equivalent duration is defined in terms of a single parameter n. From a study of the inelastic response of structural systems to simulated and recorded accelerograms, specific values of n are suggested. Stochastic models of earthquake motions for inelastic response analysis corresponding to typical recorded accelerograms are proposed.

GENERAL METHOD OF SIMULATION

Recent studies demonstrated that some recorded accelerograms are highly nonstationary in spectral characteristics; therefore, such spectral nonstationarity may be necessary for accurate simulation of earthquake motions. On the other hand, simple stochastic models are preferrable for obtaining the relevant response statistics. On this basis, this study follows the conventional method of representing stochastic models of ground motions; the earthquake acceleration $x(t)$ is expressed as

$$x(t) = \sigma_{max} f(t) g(t) \tag{1}$$

in which σ_{max}=maximum rms intensity, $f(t)$=nonstationary envelope function, and $g(t)$=stationary Gaussian process with a zero mean and unit variance.

[I] Associate Professor of Civil Engineering, Kyoto University, Kyoto, Japan.

[II] Professor of Civil Engineering, University of Illinois at Urbana-Champaign, Urbana, Illinois, U.S.A.

Type A: $G_n(\omega) = \dfrac{\gamma_A}{\omega_g} \dfrac{1+4\beta_g^2(\omega/\omega_g)^2}{H(\omega)}$ (5.a)

Type B: $G_n(\omega) = \dfrac{\gamma_B}{\omega_g} \dfrac{(\omega/\omega_g)^2}{H(\omega)}$ (5.b)

Type C: $G_n(\omega) = \dfrac{\gamma_C}{\omega_g} \dfrac{\omega/\omega_g}{H(\omega)}$ (5.c)

where:

$$\gamma_A = \frac{4\beta_g}{\pi(1+4\beta_g^2)} \ , \quad \gamma_B = \frac{4\beta_g}{\pi} \ , \quad H(\omega) = \{1-(\omega/\omega_g)^2\}^2 + 4\beta_g^2(\omega/\omega_g)^2$$

$$\gamma_C = \begin{cases} \dfrac{8\beta_g\sqrt{1-\beta_g^2}}{\pi} \Big/ \left(1+\dfrac{2}{\pi}\tan^{-1}\dfrac{1-2\beta_g^2}{2\beta_g\sqrt{1-\beta_g^2}}\right) \ ; & 1 > \beta_g > 0 \\[3mm] 2 \ ; & \beta_g = 1 \\[3mm] 4\beta_g\sqrt{\beta_g^2-1} \Big/ \ln\{(\beta_g+\sqrt{\beta_g^2-1})/(\beta_g-\sqrt{\beta_g^2-1})\} \ ; & \beta_g > 1 \end{cases}$$

and ω_g, and β_g are frequency and shape parameters of the spectral functions. If the peak frequency f_p is given, ω_g is represented by

Type A: $\omega_g = 4\pi\beta_g f_p \Big/ \sqrt{\sqrt{1+8\beta_g^2}-1}$ (6.a)

Type B: $\omega_g \doteq 2\pi f_p$ (6.b)

Type C: $\omega_g = 2\pi\sqrt{3/(1-2\beta_g^2+2\sqrt{1-\beta_g^2+\beta_g^4})} \ f_p$ (6.c)

These functions were least-square fitted to the squared Fourier amplitude spectra of recorded accelerograms normalized to have unit areas. Two dimensional least-square fitting was used with varying peak frequency f_p and shape parameter β_g, and the best-fitting spectral function was selected. The type of function, and the values of the parameters f_p and β_g are shown in Table 1 and Fig.4. No single function of the three seems to be able to represent all types of accelerogram. Within the accelerograms analyzed in this study, the choice among the three seems to depend on the value of the peak frequency; as f_p increases, the optimum spectral function changes from type C to type A.

INELASTIC STRUCTURAL RESPONSE TO SIMULATED AND RECORDED ACCELEROGRAMS

Each of the recorded accelerograms listed in Table 1 was modeled by a sample function of the proposed simulated earthquake motion. The simulated and recorded accelerograms were then compared in terms of the deformation spectra and the dissipated hysteretic energy for elastoplastic systems, for various values of undamped natural frequency f_o and ductility factor μ. A viscous damping of 2% critical was used throughout.

Fig.5 shows examples of the deformation spectra for the 1940 El Centro and corresponding simulated accelerograms. In this case, the simulated motions are generated with stationary envelope, whose equivalent duration coincides with its total duration. As a consequence, it is observed in Fig.5 that as n increases the deformation spectra for the simulated accelerogram decreases relative to those for the recorded accelerogram. This effect is particularly pronounced in the lower frequency region.

Sample functions of the stationary process $g(t)$ with a prescribed power spectral density $G_n(\omega)$ are generated by superposing harmonic components as proposed by Shinozuka and Jan (5). The generated artificial accelerograms were segmentally corrected for baseline (4) in order to assure zero starting velocity and displacement.

NONSTATIONARITY PARAMETERS

The nonstationary envelope of recorded accelerograms is obtained by taking the square root of the weighted moving average of the squared acceleration. A sinusoidal window function as shown in Fig.1 is used. From a numerical study, an averaging interval of 4 sec appears satisfactory. The resulting time function is normalized with respect to the maximum rms intensity σ_{max}, which is the nonstationary envelope function $f(t)$ for the record. Values of σ_{max} are shown in Table 1, and an example of $f(t)$ is shown in Fig.2(a).

The equivalent duration of the ground motion is defined by

$$T_n = \int_0^\infty \{f(t)\}^n dt \qquad (2)$$

in which n is an arbitrary parameter. As n increases, the strongest part of the accelerogram contributes increasingly to the integral in Eq.2, thus decreasing the value of T_n as shown in Fig.3.

Two types of nonstationary envelope function were used; one is the envelope proposed by Amin and Ang (1) and the other is a simple stationary envelope. The parameters for these functions are adjusted so that they have the same equivalent duration as the corresponding recorded accelerograms. The two envelope functions are expressed as follows:

Amin-Ang envelope: $\quad f(t) = \begin{cases} 0 & ; \quad t < 0 \\ (t/t_1)^2 & ; \quad 0 \leq t \leq t_1 \\ 1 & ; \quad t_1 \leq t \leq t_2 \\ e^{-c(t-t_2)} & ; \quad t \geq t_2 \end{cases} \qquad (3.a)$

stationary envelope: $\quad f(t) = \begin{cases} 1 & ; \quad 0 \leq t \leq t_3 \\ 0 & ; \quad t < 0, \ t > t_3 \end{cases} \qquad (3.b)$

The parameters t_1, t_2, t_3 are determined from the following:

$$\left. \begin{array}{l} t_1 = 1.5\text{sec}, \quad t_2 = T_n + \dfrac{3n}{2n+1} - \dfrac{1}{0.18n} \ (\text{sec}), \quad c = 0.18\text{sec}^{-1}, \\[2mm] \qquad\qquad \text{if} \quad T_n \geq \dfrac{1.5}{2n+1} + \dfrac{1}{0.18n} \ (\text{sec}); \\[4mm] t_1 = t_2 = T_n/(\dfrac{1.5}{2n+1} + \dfrac{1}{0.27n}) , \quad c = \dfrac{0.27}{t_1} , \\[2mm] \qquad\qquad \text{if} \quad T_n < \dfrac{1.5}{2n+1} + \dfrac{1}{0.18n} \ (\text{sec}); \text{ and} \\[2mm] t_3 = T_n \end{array} \right\} \qquad (4)$$

Examples of these envelope functions are shown in Fig.2(b).

SPECTRAL SIMULATION

The following three types of single-peaked spectral functions were examined.

The error in the deformation spectra of the simulated motions were evaluated in terms of the natural logarithm of the ratio of the simulated deformation spectra V_s to the recorded spectra V_r, $r_d = \ln(V_s/V_r)$. The error in the dissipated hysteretic energy was evaluated in similar term, i.e., $r_e = \ln(E_s/E_r)$ where E_s and E_r are hysteretic energies for the simulated and recorded accelerograms, respectively. Fig.6 shows the mean error in the deformation spectra $\bar{r}_d$ for the twelve accelerograms of Table 1. Observe that $\bar{r}_d$ does not vary greatly with the ductility factor μ. Although $\bar{r}_d$ decreases with n, it is sensitive to n only in the low-frequency range. On the other hand, from Fig.7 which shows the mean error $\bar{r}_e$ in the hysteretic energy, the simulation errors vary more significantly with n.

ACCEPTABLE RANGE OF n AND PROPOSED MODELS OF EARTHQUAKE MOTION

Within the numerical results examined in this study, it is difficult to find a single value of n that will give $\bar{r}_d \approx 0$ and $\bar{r}_e \approx 0$ for all values of frequency. However, if we admit an allowable mean simulation error of ± 0.5 in $\bar{r}_d$ and $\bar{r}_e$, then acceptable ranges of n can be established as shown in Fig.8. Note that the acceptable range of n for the Amin-Ang envelope is generally wider than that for the stationary envelope. This has been achieved by modeling the initial transient phase and the subsiding tail in the Amin-Ang envelope. In this regard, the Amin-Ang envelope has advantage over the stationary envelope.

To assure wide applicability of the equivalent duration defined by Eq.2, acceptable values of n common for both types of envelope functions are adopted. From Fig.8, any value of n between 1 and 2 is acceptable for wide ranges of frequency 0.1 to 10 Hz, if only the deformation spectra or the maximum responses are of interest. In contrast, if a more detailed inelastic response including hysteretic energy is required, the acceptable range of n becomes much narrower; specifically, a value of $n=1.5$ seems appropriate.

Based on the above result, time parameters t_1, t_2, and t_3 in Eq.4 characterizing the nonstationary envelope functions of simulated motions were obtained for $n = 1$, 1.5, and 2 for corresponding accelerograms. The results are shown in Table 1.

REFERENCES

1. Amin, M., and Ang, A. H-S., "Nonstationary Stochastic Model of Earthquake Motions," Journal of the Engineering Mechanics Division, ASCE, Vol.94, No.EM2, Proc. Paper 5906, Apr., 1968, pp.559-583.
2. Iyengar, R. N., and Iyengar, K. T. S. R., "Nonstationary Random Process Model for Earthquake Accelerograms," Bulletin of the Seismological Society of America, Vol.59, No.3, June, 1969, pp.1163-1188.
3. Jennings, P. C., Housner, G. W., and Tsai, N. C., "Simulated Earthquake Motions for Design Purposes," Proceedings, 4th World Conference on Earthquake Engineering, Santiago, Chile, Jan., 1969, Vol.1, pp.145-160.
4. Moraz, B., Hall, W. J., and Newmark, N. M., "A Study of Vertical and Horizontal Earthquake Spectra," Nathan M. Newmark Consulting Engineefing Services, Urbana, Illinois, Dec., 1972.
5. Shinozuka, M., and Jan, C.-M., "Digital Simulation of Random Process and Its Applications," Journal of Sound and Vibration, Vol.25, No.1, 1972, pp.111-128.
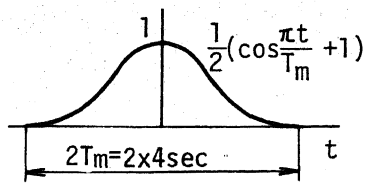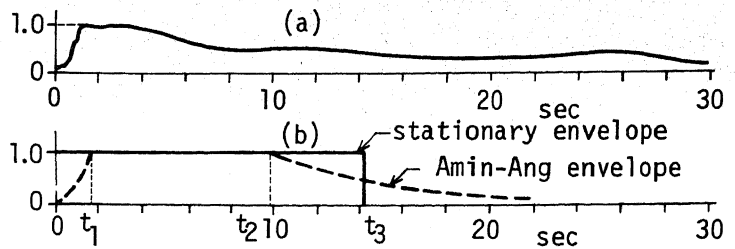
Fig.1 Window Function

$$\frac{1}{2}(\cos\frac{\pi t}{T_m}+1)$$

2Tm=2x4sec

Fig.2 Nonstationary Envelope Functions
(El Centro S00E; n=1, T_1=14.2sec)

—stationary envelope
Amin-Ang envelope

Fig.3 Equivalent Duration

Numbers correspond to Nos. in Table 1.
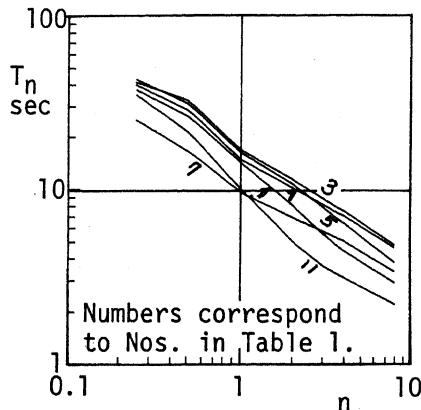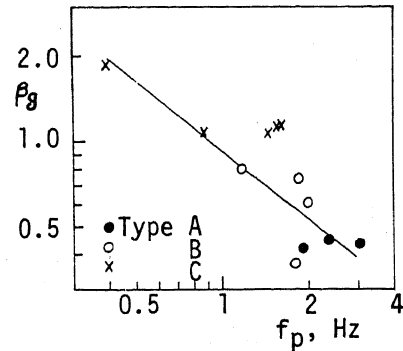
Fig.4 Parameters for Spectral Function

•Type A
oType B
×Type C
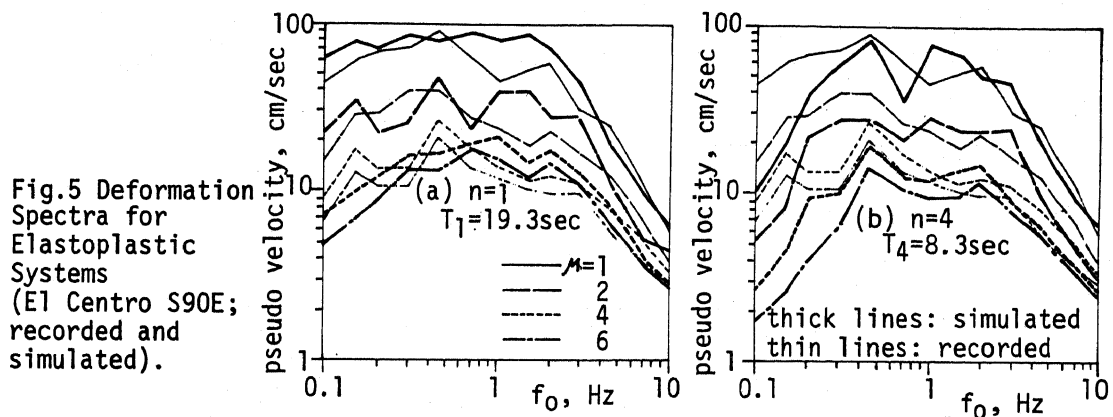
Fig.5 Deformation Spectra for Elastoplastic Systems (El Centro S90E; recorded and simulated).

(a) n=1 T_1=19.3sec
——μ=1
—— 2
------ 4
—·— 6

(b) n=4 T_4=8.3sec
thick lines: simulated
thin lines: recorded

Table 1. Recorded Accelerograms and Parameters for Simulation Model

No.	Site	Date	Comp.	Max. acc. (gal)	Type in Eq.5	f_p (Hz)	β_g	σ_{max} (gal)	n=1 t_2	n=1 $t_3=T_1$	n=1.5 t_2	n=1.5 $t_3=T_{1.5}$	n=2 t_2	n=2 $t_3=T_2$
1	El	5-08-40	S00E	342	B	1.19	0.80	114.0	9.6	14.2	7.7	10.3	6.6	8.2
2	Centro		S90W	210	A	1.91	0.42	74.8	14.7	19.3	13.6	15.6	12.1	13.7
3	Taft	7-21-52	N21E	153	C	1.46	1.08	52.1	12.2	16.8	10.8	13.4	9.9	11.5
4			S69E	176	A	2.37	0.45	58.1	10.8	15.4	9.4	12.0	8.4	10.0
5	Olympia	4-13-49	N04W	162	C	1.59	1.13	64.3	11.7	16.3	10.2	12.8	9.2	10.8
6			N86E	275	A	3.03	0.43	69.2	14.3	18.9	13.4	16.0	12.7	14.3
7	Pacoima	2-09-71	S16E	1148	C	1.63	1.14	270.9	5.0	9.6	5.3	7.9	5.3	6.9
8	Dam		S74W	1055	B	2.01	0.61	266.4	4.8	9.4	5.0	7.6	5.0	6.6
9	Orion	2-09-71	N00W	250	C	0.88	1.08	87.0	10.1	14.7	9.2	11.8	8.6	10.2
10	Blvd.		S90W	132	C	0.40	1.89	52.4	14.4	19.0	13.6	16.2	13.1	14.7
11	Castaic	2-09-71	N21E	309	B	1.85	0.74	88.6	5.0	9.6	4.0	6.6	3.5	5.1
12			N69W	265	B	1.82	0.37	92.0	7.5	12.1	6.1	8.7	5.3	6.9
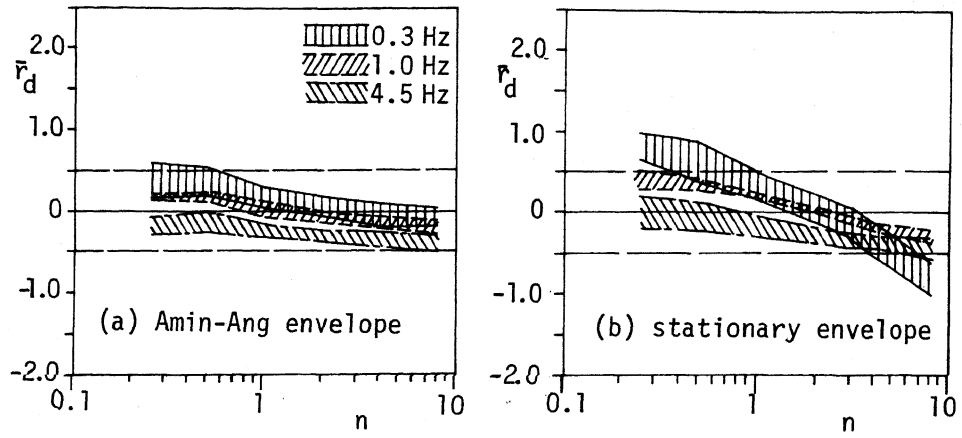
Fig.6 Simulation Error in Deformation Spectra $(\mathcal{M}=1\sim 6)$
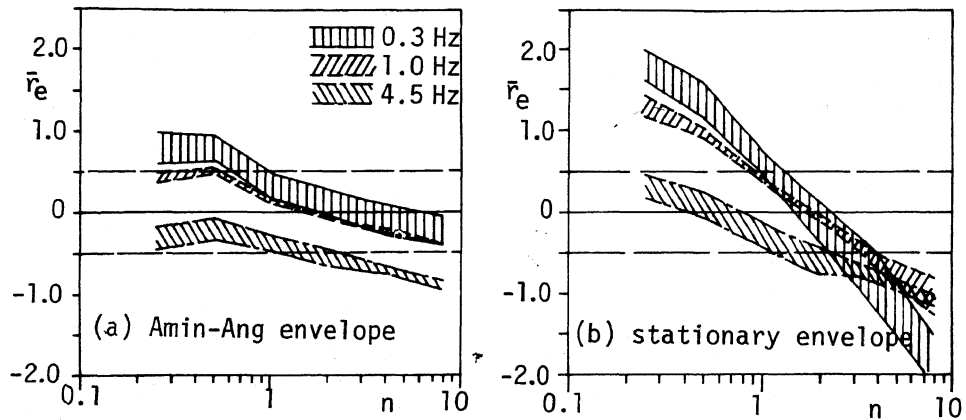
Fig.7 Simulation Error in Hysteretic Energy $(\mathcal{M}=2\sim 6)$
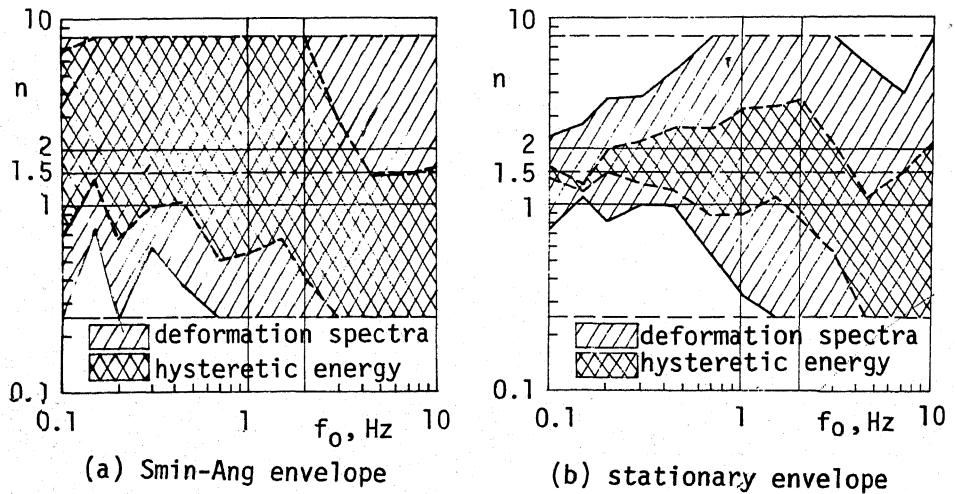

(a) Smin-Ang envelope   (b) stationary envelope

Fig.8 Acceptable Range of n